The Astrophysical Journal, 678:L101–L104, 2008 May 10
© 2008. The American Astronomical Society. All rights reserved. Printed in U.S.A.

THE ENERGY OUTPUT OF THE UNIVERSE FROM 0.1 TO 1000 μm

Simon P. Driver,[1] Cristina C. Popescu,[2] Richard J. Tuffs,[3] Alister W. Graham,[4] Jochen Liske,[5] and Ivan Baldry[6]
Received 2008 February 21; accepted 2008 March 26; published 2008 April 22

ABSTRACT

The dominant source of electromagnetic energy in the universe today (over ultraviolet, optical, and near-infrared wavelengths) is starlight. However, quantifying the amount of starlight produced has proved difficult due to interstellar dust grains that attenuate some unknown fraction of the light. Combining a recently calibrated galactic dust model with observations of 10,000 nearby galaxies, we find that (integrated over all galaxy types and orientations) only 11% ± 2% of the 0.1 μm photons escape their host galaxies; this value rises linearly (with log λ) to 87% ± 3% at 2.1 μm. We deduce that the energy output from stars in the nearby universe is (1.6 ± 0.2) × 10^{35} W Mpc^{-3}, of which (0.9 ± 0.1) × 10^{35} W Mpc^{-3} escapes directly into the intergalactic medium. Some further ramifications of dust attenuation are discussed, and equations that correct individual galaxy flux measurements for its effect are provided.

Subject headings: dust, extinction — galaxies: fundamental parameters — galaxies: photometry — galaxies: spiral — galaxies: structure

Online material: color figures

1. INTRODUCTION

The cosmic spectral energy distribution (CSED; e.g., Primack et al. 2005) provides a description of the current total (electromagnetic) energy output of the universe over all wavelengths. In the ultraviolet, optical, and near-infrared wavebands the CSED is dominated by starlight, and its measurement can be used to constrain the current stellar mass density and cosmic star formation rate as well as models of galaxy formation (e.g., Baldry & Glazebrook 2003; Hopkins & Beacom 2006). The CSED is measured by constructing the galaxy luminosity function (GLF) (Schechter 1976; Felten 1977; Driver et al. 2005) at a specified wavelength (or bandpass). The first moment of the GLF (extrapolated to bright and faint magnitudes) gives the total luminosity density at this wavelength and hence provides a single datum on the CSED.

Constructing the full CSED therefore requires accurate measurements of the GLF in a variety of bandpasses. However, galaxies contain dust, which, while negligible in terms of mass (Driver et al. 2007), attenuates some unknown fraction of the starlight before it exits a galaxy into the intergalactic medium (IGM) (Seares 1931; Giovanelli et al. 1995). The severity of this effect has proved difficult to quantify (Disney et al. 1989; Valentijn 1990; Burstein et al. 1991), leading to large uncertainties in individual galaxy flux measurements and consequently a systematic underestimation of the luminosity density (or individual CSED measurements). The degree to which the CSED is underestimated will, of course, be wavelength dependent (Cardelli et al. 1989; Calzetti 2001), and it will depend critically on the amount and distribution of the interstellar dust grains within the host galaxy (and an individual galaxy's orientation to our line of sight).

Since the heated debate of the 1990s, direct evidence from a number of methods has led to the perspective that galaxies are predominantly optically thin (at least in their outer regions). In particular, evidence from overlapping galaxies (White et al. 2000) has strongly supported the stance that galaxies are optically thin, at least in the interarm regions (Holwerda et al. 2007). Further detailed modeling of extensive optical data on edge-on galaxies also appeared to support the view that galaxies were optically thin throughout (Xilouris et al. 1999). However, the optically thin case has proved difficult to reconcile with the observed high level of far-infrared emission that is presumed to arise from dust reradiating the attenuated starlight (Bianchi et al. 2000; Popescu et al. 2000; Misiriotis et al. 2001). The resolution to this conflict may lie in a more complex dust distribution whereby galaxies may contain both optically thick (core and arm) regions and optically thin (interarm and outer) regions. Tuffs et al. (2004) and Popescu et al. (2000) (hereafter TP) have advocated a three-component dust model (optically thick inner disk, thin outer disk, and clumpy components) that is capable of reproducing the detailed multiwavelength surface photometry from UV to far-IR of edge-on galaxies such as NGC 891 and the other galaxies modeled by Xilouris et al. (1999).

Recently, Driver et al. (2007) identified evidence for strong and inclination-dependent attenuation in a large sample of disks and bulges that is not anticipated (or reproducible) in models with a purely optically thin dust distribution (e.g., see Fig. 5 in Popescu & Tuffs 2007). Similar and related results, albeit lacking bulge-disk decompositions, have also now been reported for Sloan Digital Sky Survey (SDSS) data (e.g., Choi et al. 2007; Shao et al. 2007; Unterborn & Ryden 2008; Maller et al. 2008; Padilla & Strauss 2008). Using the TP model, we were able to reproduce the attenuation-inclination relation for both disks and bulges and to constrain the mean *central B*-band face-on opacity (the only free parameter) for the galaxy population at large: $\tau_B^f = 3.8 \pm 0.7$. In this Letter we explore the implications of this result on estimates of the CSED and ask whether the high value for the central opacity can be reconciled with the far-IR output from the nearby galaxy popu-

[1] Scottish Universities' Physics Alliance (SUPA), School of Physics and Astronomy, University of St Andrews, North Haugh, St Andrews, Fife KY16 9SS, UK; spd3@st-and.ac.uk.

[2] Centre for Astrophysics, University of Central Lancashire, Preston PR1 2HE, UK.

[3] Max-Planck-Institut für Kernphysik, Saupfercheckweg 1, 69117 Heidelberg, Germany.

[4] Centre for Astrophysics and Supercomputing, Swinburne University of Technology, Hawthorn, Victoria 3122, Australia.

[5] European Southern Observatory, Karl-Schwarzschild-Strasse 2, 85748 Garching, Germany.

[6] Astrophysics Research Institute, Liverpool John Moores University, Twelve Quays House, Egerton Wharf, Birkenhead CH4 1LD, UK.

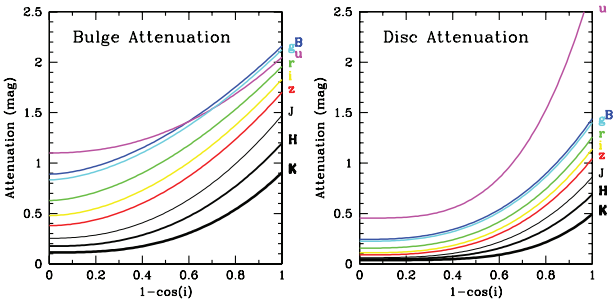

FIG. 1.—The dust attenuation-inclination relations for galaxy disks (*right*) and bulges (*left*) shown for a variety of bands (as indicated on the right-hand sides) as predicted by the TP model calibrated on *B*-band disk data (Driver et al. 2007). The nonzero attenuation at $1 - \cos(i) = 0$ is the residual face-on attenuation predicted by the model.

lation. Throughout we adopt a standard flat cosmology with $\Omega_M = 0.3$, $\Omega_\Lambda = 0.7$, and $H_0 = 70\ h_{70}$ km s^{-1} Mpc^{-1}.

2. DUST AND ITS IMPACT ON GALAXY PHOTOMETRY

The dust model we adopt here is described fully in a sequence of papers (Popescu et al. 2000; Tuffs et al. 2004; Möllenhoff et al. 2006) and is summarized by Popescu & Tuffs (2007). In brief, the model incorporates three distinct components: an extended optically thin dust disk associated with the neutral hydrogen and older stellar population (i.e., the outer disk and interarm regions), a less extended optically thick dust layer in the spiral arms associated with the molecular hydrogen and younger stellar population (i.e., primarily the inner disk), and a clumpy component (representing star-forming molecular clouds). Ideally, the optically thick component should be distributed according to a spiral pattern, to better mimic the observed variation in opacity between arm and interarm regions. For the purposes of this work this distinction, between an additional disk of uniform opacity or one with a built-in spiral density pattern, is not particularly relevant as both imply a uniform high-opacity disk in the central bulge-dominated regions.

In Driver et al. (2007) we constrained the TP model's single free parameter, the central face-on opacity in *B*, which was found to be $\tau_B^f = 3.8 \pm 0.7$. Briefly, this constraint was obtained by measuring the luminosity functions of galaxy bulges and disks at various inclinations and comparing the dependence of the turnover point on inclination [i.e., the M^*–cos (i) relation] to predictions of the TP model (see Driver et al. 2007 for full details).

Having constrained the TP model, we can now determine the inclination-dependent attenuation correction at any wavelength. From Figure 1 we see that the attenuation for bulge starlight can be as high as 2 *B* mag (i.e., only 6% of the photons escape) and as high as 1.2 *B* mag for disks (i.e., only 33% of the photons escape), depending on wavelength and inclination. While the level of attenuation of the disk is relatively consistent with previous estimates, the bulge attenuation is a surprise and has not previously been considered in detail. This is because while bulges are traditionally considered to be dust free, like elliptical galaxies, the dust in the galaxy disk attenuates bulge light, particularly from the far side. We can parameterize the dust attenuation curves of Figure 1 as follows:

$$M^c_{\rm bulge} = M^o_{\rm bulge} - b_1 - b_2[1 - \cos(i)]^{b_3}, \quad (1)$$

$$M^c_{\rm disk} = M^o_{\rm disk} - d_1 - d_2[1 - \cos(i)]^{d_3}, \quad (2)$$

TABLE 1

COEFFICIENTS FOR USE IN EQUATIONS (1) AND (2) TO PROVIDE BULGE AND DISK ATTENUATION CORRECTIONS (WITH <5% ERROR IN THE PREDICTED VALUES DUE TO THE ADOPTED FITTING FUNCTION)

Bandpass	b_1	b_2	b_3	d_1	d_2	d_3
u	1.10	0.95	2.18	0.45	2.31	3.42
B	0.89	1.27	1.73	0.24	1.20	2.73
g	0.83	1.29	1.71	0.22	1.18	2.74
r	0.63	1.33	1.73	0.16	1.10	2.80
i	0.48	1.35	1.84	0.11	1.03	2.89
z	0.38	1.35	1.84	0.09	0.96	2.98
J	0.25	1.22	2.26	0.06	0.80	3.21
H	0.18	1.02	2.43	0.05	0.64	3.51
K	0.11	0.79	2.77	0.04	0.46	4.23

where M^o and M^c represent the observed and corrected magnitudes, respectively, i is the disk inclination, and the coefficients b_1, b_2, b_3 and d_1, d_2, d_3 are listed in Table 1.

Using the Millennium Galaxy Catalogue data (MGC; Liske et al. 2003; Driver et al. 2005; Allen et al. 2006), we now derive the total *B*-band GLF incorporating the impact of dust attenuation. This involves separating all galaxies into their bulges and disk components, correcting their fluxes according to the formulae above, and then rederiving their combined fluxes (note that pure elliptical systems are not modified). Figure 2 shows the raw observed GLF (*red dotted line*), the inclination-corrected GLF (*green dashed line*), and the fully dust-corrected GLF (*blue solid line*; i.e., corrected for both the empirically verified inclination-dependent attenuation plus the residual face-on attenuation determined by the model). The corresponding Schechter function fits to the GLFs, obtained using a standard stepwise maximum likelihood estimator (Efstathiou et al. 1988), are also shown in Figure 2 and tabulated in Table 2. The changes due to the dust correction are significant. Going from the original, observed *B*-band GLF to the final, fully dust-corrected GLF, we find a 19 σ shift in the characteristic luminosity (M^*) and a 5 σ change in the faint-end slope (which determines the space density of dwarf galaxies). Nearby galaxies therefore produce far more photons in the 400–450 nm range (*B* band) than previously supposed. In fact, after first removing the contribution to the GLF due to ellipticals ($0.14h_{70}\ L_\odot$ Mpc^{-3}; Driver et al. 2005), only 58% $\pm$ 5% of *B*-band photons escape from the nearby spiral galaxy population into the IGM (or 60% $\pm$ 5% if one includes the ellipticals).

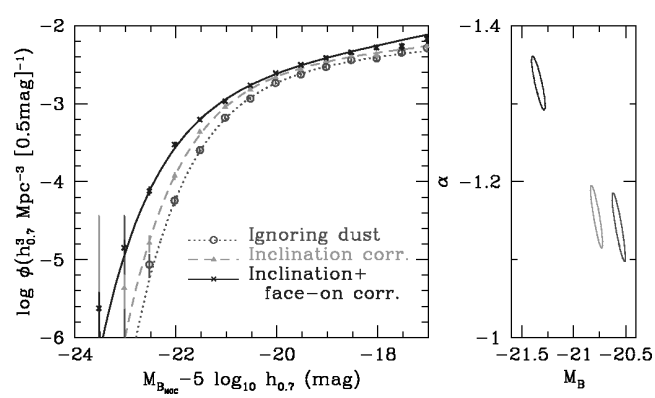

FIG. 2.—*Main panel:* The *B*-band galaxy luminosity function: ignoring all consideration of dust (*dotted line*), after consideration of the empirically derived attenuation-inclination relation only (*dashed line*), and after a full treatment of dust attenuation (including the face-on model correction; *solid line*). *Side panel:* The projected 3 σ error contours for two of the three fitting parameters, α (the faint-end slope) and M^* (the characteristic luminosity). [*See the electronic edition of the Journal for a color version of this figure.*]

TABLE 2
Derived Schechter Luminosity Function Parameters for the MGC with Varying Degrees of Dust Attenuation Corrections

Sample	$M^* - 5 \log h_{70}$ (mag)	α	ϕ_* ($10^{-3} h_{70}^3$ Mpc^{-3} [0.5 mag]$^{-1}$)	j_B ($10^8 h_{70}$ $L_\odot$ Mpc^{-3})
No dust correction	-20.57 ± 0.04	-1.14 ± 0.03	6.7 ± 0.3	1.9 ± 0.2
Inclination correction	-20.78 ± 0.04	-1.16 ± 0.03	7.0 ± 0.3	2.4 ± 0.2
Inclination+face-on correction	-21.32 ± 0.05	-1.32 ± 0.02	4.8 ± 0.3	3.1 ± 0.5

2.1. *Extrapolating the Impact of Dust on the GLF to Other Bandpasses*

The above result provides us with a single dust-corrected datum for the CSED. Unfortunately, we cannot repeat this measurement at other wavelengths because we lack the appropriate imaging data at this time. We can, however, resort to a simplification: For all possible bulge-to-total (B/T) values from 0 to 0.8, we derive, using the equations given above, the implied photon escape fraction integrated over cos (i). We then adopt as the effective mean B/T that model galaxy whose photon escape fraction is the same as that determined from our GLF analysis. This yields an intrinsic $\langle B/T \rangle = 0.13^{+0.22}_{-0.13}$. Essentially, this is an effective average B/T value that corresponds to the volume- and luminosity-weighted average of the individual escape fractions of all the galaxies in our sample in the absence of dust.

The above has provided us with an effective average galaxy that represents the galaxy population at large in the B band. To now derive the equivalent effective average galaxy at other wavelengths, we need to know the mean bulge and disk colors in order to modify the bulge-to-total ratio accordingly. For example, galaxy bulges are typically red (relative to the disk), so as we move toward longer wavelengths we expect the canonical $\langle B/T \rangle$ ratio to rise a little. To obtain the mean bulge and disk colors, we supplement our B-band MGC data with multiwavelength data provided by the overlapping SDSS (Driver et al. 2005, 2007; Liske et al. 2003; Allen et al. 2006). Using the median colors for bulge-only or disk-only systems, we transpose our canonical bulge-to-total ratio to the SDSS bandpasses: $\langle B/T \rangle = 0.11$ (u), 0.14 (g), 0.14 (r), 0.14 (i), 0.16 (z). For JHK we adopt the z-band $\langle B/T \rangle$ ratio, and for the UV range we adopt $\langle B/T \rangle = 0$ (which implicitly assumes that star formation has ceased in the bulge regions).

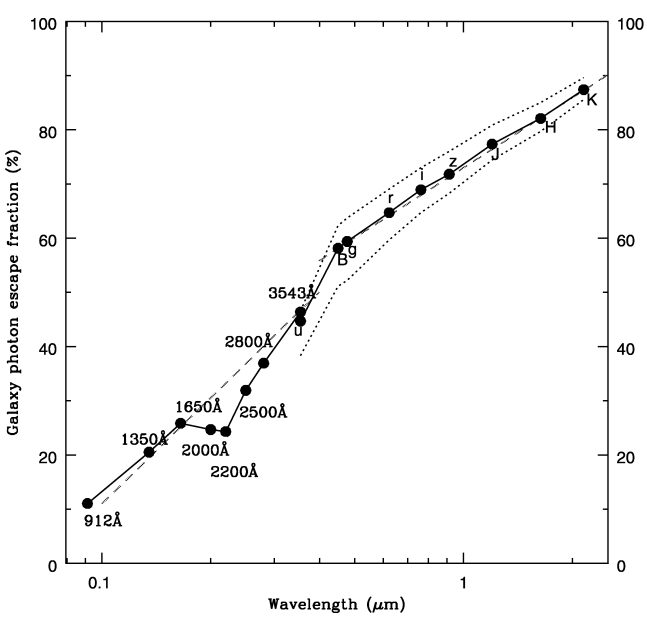

Fig. 3.—The global photon escape fraction averaged over all inclinations vs. wavelength. The dotted lines show estimated error boundaries (see text). [*See the electronic edition of the Journal for a color version of this figure.*]

2.2. *The Photon Escape Fraction*

We can now derive the mean photon escape fraction at any wavelength using the bulge and disk attenuation-inclination relations predicted by our calibrated dust model (see § 2) coupled with the above $\langle B/T \rangle$ values. Figure 3 displays the corresponding photon escape fractions for a variety of bandpasses averaged over all viewing angles. To understand how critically this depends on the adopted $\langle B/T \rangle$ values, we also show in Figure 3 the photon escape fractions that result from assuming, in each bandpass, the extreme values of $\langle B/T \rangle = 0$ (pure disk; *upper dotted line*) and $\langle B/T \rangle = 0.35$ (early/mid-type disk galaxy; *lower dotted line*), respectively. Evidently, the photon escape fractions do not depend critically on the assumed "canonical" values of $\langle B/T \rangle$, and hence our shortcut method should be considered robust (i.e., Fig. 3 is essentially a direct prediction from the MGC calibrated dust model with little dependence on $\langle B/T \rangle$).

2.3. *The Cosmic Energy Spectrum*

The values shown in Figure 3 can be used to derive the CSED corrected for dust attenuation. A compendium of recent GLF measurements (Driver et al. 2007; Budavari et al. 2005; Blanton et al. 2003; Kochanek et al. 2001; Bell et al. 2003; Babbedge et al. 2006; Huang et al. 2007; Takeuchi et al. 2006) based on nearby samples (all allegedly complete, corrected to redshift 0, and converted to $H_0 = 70$ km s^{-1} Mpc^{-1}, but uncorrected for dust attenuation) are shown in Figure 4. Where necessary these have been converted from luminosity density units to energy density units, and together they span the wavelength range from the far-UV to the far-IR. Also shown in Figure 4 is our single fully dust-corrected B-band luminosity density value (from Table 2), which lies significantly above the previous uncorrected estimates.

Using the photon escape fractions from Figure 3, we now correct the attenuated GLF measurements to produce, for the first time, the unattenuated CSED (Fig. 4, *gray data points*). This constitutes the actual spectral energy output in the universe today due to the total integrated starlight before dust attenuation. To calculate the total energy of starlight versus that which escapes into the IGM, we need to integrate over these two data sets. In order to interpolate across the full far-UV, optical, and IR wavelength range, we adopt a recent stellar synthesis model (PEGACE; Fioc & Rocca-Volmerange 1997; see Baldry & Glazebrook 2003 for details of the modeling) that provides a reasonable fit to both the attenuated (*orange line*) and, when corrected, unattenuated (*black line*) CSED. Integrating these two curves yields a total stellar energy output of $(1.6 \pm 0.2) \times 10^{35}$ W Mpc^{-3}, of which $(0.9 \pm 0.1) \times 10^{35}$ W Mpc^{-3} escapes into the IGM. Note that these numbers take into account a 10% component of the CSED longward of 400 nm due to ellipticals (Driver et al. 2005). For the CSED to be in equilibrium (and energy conserving), the difference between these two energy values, $(0.7 \pm 0.2) \times 10^{35}$ W Mpc^{-3}, should not

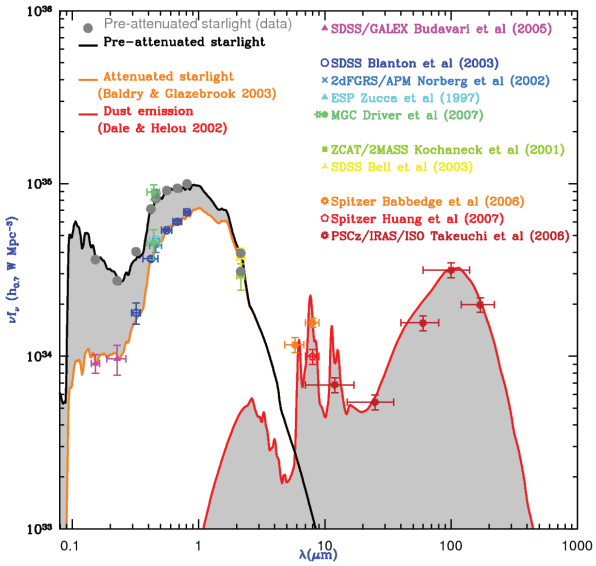

FIG. 4.—The cosmic energy output covering the region dominated by starlight (*left peak*) and by dust emission (*right peak*). The orange line shows the observed (uncorrected) cosmic energy output from the total nearby galaxy population, while the black line shows the same after correction for the fraction of photons attenuated by dust. The discrepancy in the integrals over these two curves yields the total energy of starlight lost to heating of the dust grains. If starlight is the only source of dust heating, then this energy loss must equal the total radiant energy of the dust emission (i.e., the two shaded regions must and do contain equal energy).

exceed the total emission from dust in the far-IR, the traditional sticking point for optically thin models. Figure 4 also shows a model of the dust emission (*red line*; Dale & Helou 2002) that reproduces fairly well the observed data. Integrating the far-IR curve, we obtain a total radiant dust energy of $(0.6 \pm 0.1) \times 10^{35}$ W Mpc^{-3}, in excellent agreement with our prediction. This provides independent support that the high value for the central face-on opacity is correct and implies that significant corrections to the observed flux of individual galaxies are necessary. This result also leaves little or no room for other sources of dust heating in the nearby universe, such as active galactic nuclei, and provides the first fully reconciled estimate of the CSED.

3. DISCUSSIONS AND RAMIFICATIONS

This work has reconciled three apparently inconsistent observations, namely, the severe attenuation-inclination relation seen in the MGC data (Driver et al. 2007), the conclusion that interarm regions are optically thin (White et al. 2000; Holwerda et al. 2007), and the relatively high far-IR dust emission. The TP model achieves this by incorporating distinct dust components that allow for optically thin interarm and outer regions coupled with an optically thick central region. This relatively simple development has a number of far-reaching ramifications. First, all basic measurements of galaxy fluxes that do not correct for dust attenuation will require significant revision (i.e., 0.2–2.5 mag in *B*) depending on an individual galaxy's inclination, bulge-to-total ratio, and wavelength of observation. Second, many galaxies will contain heavily embedded bulges due to the centrally concentrated dust in their disks. This can easily lead to significant errors in optical estimates of their fluxes and stellar masses; this is because although stellar mass estimates do correct for optically thin dust attenuation, they cannot, of course, correct for mass hidden behind an entirely optically thick screen. Finally, dust attenuation could conceivably play a part in the morphology-density relation and the proposed transformation of disk galaxies from late to early type as they enter the cluster environment. For example, using the corrections provided, it is easy to show that an Sab galaxy at the median inclination (60°) will see its observed *B*/*T* change from 0.3 to 0.6, its color get significantly redder, and its luminosity get brighter, if all its dust were to be removed.

Richard Tuffs is grateful for the support of a Livesey Award while working on this paper at UCLan.

REFERENCES

Allen, P., Driver, S. P., Graham, A. W., Cameron, E., Liske, J., Cross, N. J. G., & De Propris, R. 2006, MNRAS, 371, 2
Babbedge, T. S. R., et al. 2006, MNRAS, 370, 1159
Baldry, I., & Glazebrook, K. 2003, ApJ, 593, 258
Bell, E., McIntosh, D., Katz, N., & Weinberg, M. D. 2003, ApJS, 149, 289
Bianchi, S., Davies, J. I., & Alton, P. B. 2000, A&A, 359, 65
Blanton, M., et al. 2003, ApJ, 592, 819
Budavari, T., et al. 2005, ApJ, 619, L31
Burstein, D., Haynes, M. P., & Faber, M. 1991, Nature, 353, 515
Calzetti, D. 2001, PASP, 113, 1449
Cardelli, J. A., Clayton, G. C., & Mathis, J. S. 1989, ApJ, 345, 245
Choi, Y., Park, C., & Vogeley, M. S. 2007, ApJ, 658, 884
Dale, D. A., & Helou, G. 2002, ApJ, 576, 159
Disney, M. J., Davies, J. I., & Phillipps, S. 1989, MNRAS, 239, 939
Driver, S. P., Liske, J., Cross, N. J. G., De Propris, R., & Allen, P. D. 2005, MNRAS, 360, 81
Driver, S. P., Popescu, C., Tuffs, R. J., Graham, A. W., Liske, J., Allen, P. D., & De Propris, R. 2007, MNRAS, 379, 1022
Efstathiou, G., Ellis, R. S., & Peterson, B. A. 1988, MNRAS, 232, 431
Felten, J. E. 1977, AJ, 82, 861
Fioc, M., & Rocca-Volmerange, B. 1997, A&A, 326, 950
Giovanelli, R., et al. 1995, AJ, 110, 1059
Holwerda, B. W., Keel, W. C., & Bolton, A. 2007, AJ, 134, 2385
Hopkins, A. M., & Beacom, J. F. 2006, ApJ, 651, 142
Huang, J.-S., et al. 2007, ApJ, 664, 840
Kochanek, C. S., et al. 2001, ApJ, 560, 566
Liske, J., Lemon, D. J., Driver, S. P., Cross, N. J. G., & Couch, W. J. 2003, MNRAS, 344, 307
Maller, A., Berlind, A. A., Blanton, M. R., & Hogg, D. W. 2008, ApJ, submitted (arXiv:0801.3286)
Misiriotis, A., Popescu, C. C., Tuffs, R. J., & Kylafis, N. D. 2001, A&A, 372, 775
Möllenhoff, C., Popescu, C. C., & Tuffs, R. J. 2006, A&A, 456, 941
Padilla, N. D., & Strauss, M. A. 2008, MNRAS, submitted (arXiv:0802.0877)
Popescu, C. C., Misiriotis, A., Kylafis, N. D., Tuffs, R. J., & Fischera, J. 2000, A&A, 362, 138
Popescu, C. C., & Tuffs, R. J. 2007, preprint (arXiv:0709.2310v1)
Primack, J., Bullock, J. S., & Somerville, R. S. 2005, in AIP Conf. Proc. 745, Observational Gamma-Ray Cosmology, ed. F. A. Aharonian, H. J. Völk, & D. Horns (New York: AIP), 22
Schechter, P. 1976, ApJ, 203, 297
Seares, F. H. 1931, PASP, 43, 371
Shao, Z., Xiao, W., Shen, S., Mo, H. J., Xia, X., & Deng, Z. 2007, ApJ, 659, 1159
Takeuchi, T. T., Ishii, T. T., Dole, H., Dennefeld, M., Lagache, G., & Puget, J.-L. 2006, A&A, 448, 525
Tuffs, R. J., Popescu, C. C., Völk, H. J., Kylafis, N. D., & Dopita, M. A. 2004, A&A, 419, 821
Unterborn, C. T., & Ryden, B. S. 2008, ApJ, submitted (arXiv:0801.2400)
Valentijn, E. A. 1990, Nature, 346, 153
White, R. E., III, Keel, W. C., & Conselice, C. J. 2000, ApJ, 542, 761
Xilouris, E. M., Byun, Y. I., Kylafis, N. D., Paleologou, E. V., & Papamastorakis, J. 1999, A&A, 344, 868